



HHS Public Access

Author manuscript

Neuroimage. Author manuscript; available in PMC 2020 February 15.

Published in final edited form as:

Neuroimage. 2019 February 15; 187: 3–16. doi:10.1016/j.neuroimage.2017.12.095.

Recent Progress in ASL

Luis Hernandez-Garcia, Anish Lahiri, and Jonas Schollenberger

Abstract

This article aims to provide the reader with an overview of recent developments in Arterial Spin Labeling (ASL) MRI techniques. A great deal of progress has been made in recent years in terms of the SNR and acquisition speed. New strategies have been introduced to improve labeling efficiency, reduce artefacts, and estimate other relevant physiological parameters besides perfusion. As a result, ASL techniques has become a reliable workhorse for researchers as well as clinicians. After a brief overview of the technique's fundamentals, this article will review new trends and variants in ASL including vascular territory mapping and velocity selective ASL, as well as arterial blood volume imaging techniques. This article will also review recent processing techniques to reduce partial volume effects and physiological noise. Next the article will examine how ASL techniques can be leveraged to calculate additional physiological parameters beyond perfusion and finally, it will review a few recent applications of ASL in the literature.

Introduction

A major goal of modern medical imaging is to move beyond qualitative images that may be informative about the shape, size and texture of tissue, and into a world where medical images are also quantitative. One of the more popular and prominent techniques is arterial spin labeling (ASL), which can produce quantitative images of perfusion. Brain perfusion (defined as the amount of blood delivered to a unit of tissue per unit of time) is a well known indicator of tissue metabolism and function. As such, it is proving to be a powerful workhorse to study brain function and gaining prominence as a clinical tool, but it is still an evolving technique.

The concept behind ASL is relatively simple: conceptually, it is very similar to tracer injection perfusion measurements (e.g., bolus tracking MRI, autoradiography, PET ...etc.) except that, instead of injecting a tracer into the blood stream and tracking its accumulation into the tissue, the tracer consists of the blood water in the arteries itself. The tracer is created by inverting the magnetization of the blood in the arteries that feed the organ of interest with a train of RF pulses. As this "labeled" blood flows into the tissue, it reduces the available magnetization in the tissue. As a result, images collected downstream of the labeling location appear slightly darker. By subtracting the labeled images from a set of

Corresponding Author: Luis Hernandez-Garcia, Ph.D., FMRI Laboratory, University of Michigan, 2360 Bonisteel Blvd., Ann Arbor, MI, 48109-2108.

Publisher's Disclaimer: This is a PDF file of an unedited manuscript that has been accepted for publication. As a service to our customers we are providing this early version of the manuscript. The manuscript will undergo copyediting, typesetting, and review of the resulting proof before it is published in its final citable form. Please note that during the production process errors may be discovered which could affect the content, and all legal disclaimers that apply to the journal pertain.

control images, we can calculate the amount of blood that entered the organ since the beginning of the labeling period. For example, the most common use of ASL is for brain perfusion imaging, is done by labeling blood just before it enters the brain through the carotid and vertebral arteries. After a brief delay, a set of “labeled” brain images is acquired. Next, a second set of “control” images is acquired identical to the first, except that this time, the labeling pulses do not invert the blood magnetization at all, but simply serve as a control for any side effects of the labeling pulses (namely magnetization transfer (Williams, Detre, Leigh, & Koretsky, 1992; Wolff & Balaban, 1989; W. Zhang, Silva, Williams, & Koretsky, 1995)). The subtraction of these two images is roughly proportional to the perfusion rate (see figure 1, depicting the ASL technique). If desired, one can acquire a time series of such image pairs in order to examine the brain’s activity during a stimulation paradigm.

The main variations of the technique have to do with the labeling scheme. One could label a large segment of the neck region with a single pulse, as in the case of Pulsed ASL techniques, or one could apply a long pulse (or a train of pulses) at a thin slice through the neck that labels the blood as it flows through it, as in the case of continuous and pseudo-continuous ASL. More recently, “velocity selective” techniques have been developed such that only moving spins are labeled, regardless of their spatial position.

In general, ASL subtraction images have been shown to be roughly proportional to the perfusion rate with the appropriate scaling factors for the specific technique. Since the invention of ASL, there have been numerous validation studies of different ASL variants and their corresponding quantification models that compared them to other independent perfusion measurements (M. a. Chappell et al., 2013; J. J. Chen, Wieckowska, Meyer, & Pike, 2008; Ewing, Cao, Knight, & Fenstermacher, 2005; Gao et al., 2014; Hartkamp et al., 2014; Ye, 2000).

While ASL was invented around the same time as the BOLD effect was discovered (Detre, Leigh, Williams, & Koretsky, 1992; Williams et al., 1992), it has only been in the last five years that ASL has been widely adopted by the neuroimaging community. Largely, this recent resurgence of ASL has come about because of a combination of technical advances. The technique was previously challenged by its inherent low signal to noise ratio (SNR), and slow temporal resolution. With the advent of parallel imaging (Blaimer et al., 2004; Deshmane, Gulani, Griswold, & Seiberlich, 2012; Pruessmann, Weiger, Scheidegger, & Boesiger, 1999), the development of pseudo-continuous labeling (Dai, Garcia, De Bazelaire, & Alsop, 2008) and background suppression schemes (Ye, Frank, Weinberger, & McLaughlin, 2000)(St. Lawrence, Frank, Bandettini, & Ye, 2005)(Garcia, Duhamel, & Alsop, 2005), ASL images can now be acquired with sufficient speed and quality to be a robust, quantitative imaging tool. Another major hurdle to the adoption of ASL was the great diversity of schemes used by different investigators. It was not until 2014, that the community came together to make a set of recommendations for the implementation of a robust variant of ASL that could be used reliably as a “standard” implementation, even if not necessarily the best possible implementation for every application. However, this has created a *de facto* standard and helped the different vendors implement an ASL pulse sequence that can be distributed as a packaged product (Alsop et al., 2015). At the time of this writing, there are efforts under way to establish gold standards for calibration and validation of ASL

images. Specifically, a profile for ASL is being created for the Quantitative Imaging Biomarkers Alliance (QIBA see <http://www.rsna.org/qiba>) that will describe a set of applications, capabilities and standards for ASL as a quantitative biomarker.

Having said that, this article will focus on recent progress in the development of ASL techniques at the time of writing. As mentioned earlier, a great deal of progress has been made in recent years on fast image acquisition techniques to boost the SNR and speed of the measurement. Additionally, new strategies have been introduced to improve labeling efficiency, reduce artefacts, and estimate other relevant physiological parameters using ASL techniques besides perfusion. As a result, a host of new applications for ASL techniques is becoming available to researchers, although we will only focus on neuroimaging applications.

Velocity and Acceleration Selective Labeling

The main challenges faced by ASL are its low signal to noise ratio (SNR) and its slow temporal and spatial resolution (Y. Chen, Wang, & Detre, 2011; Perthen, Bydder, Restom, & Liu, 2008; E C Wong, Buxton, & Frank, 1998). The low SNR is due in part to the small fraction of blood that enters a voxel. Additionally, by the time the labeled spins reach the voxel, they have relaxed significantly during transit. T1 relaxation during bolus arrival time destroys about 50% of the label. The longer the travel time, the more label is lost. The SNR challenge is most significant in the white matter (Van Gelderen, De Zwart, & Duyn, 2008) where perfusion rates are lower and arterial bolus arrival times are longer. Although feasible (Van Osch et al., 2009), white matter ASL imaging requires lengthy scans and yields images of inferior quality. As a result, white matter perfusion is often neglected or overlooked.

A solution to this problem was proposed in 1999, by the introduction of velocity-selective saturation pulses (Norris & Schwarzbauer, 1999) and demonstrated in humans (Eric C Wong et al., 2006; Wu & Wong, 2007). The concept is relatively simple: instead of inverting the spins at the feeding arteries, upstream of the target region, an arterial label can also be created *within the target region* by saturating only the moving spins (i.e., blood), thus reducing the arrival time of the label to a negligible amount. The arterial saturation was originally achieved by a 90 degree pulse that first tips the magnetization into the transverse plane, followed by two or more adiabatic 180 degree pulses surrounded by gradient pulses with a net zero moment. This results in dephasing of spins moving above a certain velocity encoding threshold, or V_{enc} , while the spins moving slower than the threshold regain phase coherence. Lastly, the magnetization is returned to the z-axis by a -90 degree pulse. Ideally, after this preparation pulse train, the arterial and venous spins are saturated while the stationary tissue spins are largely unaffected (see figure 2). In order to produce a suitable control image, the same preparation pulse train is played out again, but without the velocity encoding gradients, thus returning all the spins to the longitudinal axis. It's important to note that this preparation will be very sensitive to the flip angles obtained with each individual pulse, thus most implementations will use adiabatic pulses, which are known to be more robust to B1 inhomogeneity.

There are some drawbacks to this strategy. First, the label consisted in saturation of the arterial spins, rather than inversion, thus giving up half of the label. Second, the velocity encoding gradients generate unwanted eddy currents and diffusion weighting in the labeled image that are not present in the control image. After subtracting control and labeled images, these effects result in systematic bias in a perfusion measure. The diffusion sensitivity issue results can be particularly noticeable because the ASL subtraction image can potentially show large signals arising from the cerebrospinal fluid, completely unrelated to perfusion. Finally, the size of the labeling bolus (or input function) is not as large as in the PCASL case, reducing the SNR of the measurement.

However, steady progress has been made to alleviate these problems starting with the inclusion of adiabatic pulses (Eric C Wong et al., 2006; Wu & Wong, 2007). Using a cleverly designed composite BIR-8 pulse train (see figure 3), Guo and Meakin were able to reduce the eddy current and diffusion effects (Guo, Meakin, Jezzard, & Wong, 2014; Meakin & Jezzard, 2013) quite dramatically. Further inroads have been made by concatenating two or three such labeling pulses in order to achieve a significantly longer labeling input function and boost the SNR of the resulting ASL image (Guo et al., 2014)

Recently, Qin et al, have introduced a composite pulse train that inverts the magnetization of spins moving within a velocity band, while leaving the magnetization of other velocities largely intact. This pulse train is based on a velocity phase-encoding formalism, analogous to k-space excitation (see figure 4). One can think of it as traversing velocity k-space with a hard 180 degree pulse that is broken into equal segments. An additional set of refocusing 180 degree pulses is added to refocus off-resonance effects along the way. As a result, they demonstrated that the technique could produce ASL images rivaling PCASL in terms of SNR, but without the sensitivity to bolus arrival time variations. This group has also been able to dramatically improve the quality of non-contrast angiography using this technique (Qin et al., 2015; Qin & van Zijl, 2016).

An interesting issue in velocity selective labeling is that arterial blood is known to decelerate significantly as it enters the brain. This can lead to some challenges (i.e., errors in velocity selectivity) but also opportunities. Using a similar strategy to velocity encoding, acceleration selective labeling was demonstrated by Schmid et al. (Obara et al., 2016; Schmid, Heijtel, et al., 2014; Schmid, Ghariq, Teeuwisse, Webb, & Van Osch, 2014). Acceleration encoding can be done using similar principles as in the velocity encoding case, but the encoding is done by designing the gradient pulses such that their zeroth and their first order moments equal zero. In the case of the original implementation by Schmid et al (Schmid, Ghariq, et al., 2014), converting the pulse from velocity to acceleration selective was just a matter of reversing the sign of two of the gradient lobes.

Velocity and Acceleration selective labeling are, at the time of writing, still areas of active research and development and we expect to see new variants and applications in the near future.

Vascular territory imaging (VTI)

Knowledge of cerebral perfusion territories can provide significant information in clinical cases where the vascular tree is compromised (e.g. carotid stenosis, intracranial arteriovenous malformation) and knowledge of collateral blood supply to each region is necessary. “Vessel-selective” labeling can be achieved by modifying the PCASL scheme to invert only the blood traveling through specific sub-regions of the labeling plane. A recent example of vessel selective ASL can be seen in a study by Richter et al., in which the technique was used to examine the reorganization of blood flow supply following stenotic disease (Richter et al., 2017). Currently available approaches of VTI generally rely on the application of additional gradient pulses along the labeling plane between RF pulses, in combination with a linear phase shift to the RF pulse train (see Figure 5). The additional in-plane gradients cause flowing spins to accumulate an extra phase shift, ϕ , depending on their location within the labeling plane:

$$\Delta\phi_k = \gamma(G_{z,ave} \cdot z \cdot \Delta t + G_{0,x,k} \cdot x + G_{0,y,k} \cdot y) \quad [1]$$

Where γ is the gyromagnetic ratio; $G_{z,ave}$ is the mean slice-selective gradient; $G_{0,x,k}$ and $G_{0,y,k}$ are the zeroth moments of the transverse x- and y gradients at the kth RF pulse; x, y, and z denote the label position relative to the isocenter. The phase of the next RF pulse must then be adjusted to match the phase gain at the desired location. As a result, only spins in the desired location (with the right amount of phase) maintain the spin lock condition and become inverted.

Vessel-encoded pcasl (ve-pcasl), as first introduced by Wong (Eric C. Wong, 2007), uses constant gradients to generate a periodic banding pattern along the labeling plane where the flowing spins are inverted. Thus, two separate vessels can be in a tag and a control region, respectively by adjusting the in-plane gradient such that there is a 180 degree phase shift between them (see the left panel of figure 6). By extension of this concept, a Hadamard encoding scheme can be used to label different combinations of vessels over several ASL image acquisitions. The perfusion contributions from individual vessels to each voxel can be calculated from the resulting images by inverting the Hadamard encoding matrix.

In order to avoid time-consuming calibration of the labeling scheme to the subject’s anatomy and to facilitate clinical use, a “planning-free” application of ve-pcasl has gained popularity. Based on a population-averaged vessel anatomy, a standardized set of vessel-encoding steps can be derived. Instead of carefully placing the label and control stripes on the target vessels, a fixed gradient amplitude and orientation, as well as phase shift is assumed for all subjects. Subsequently, the individual vessels’ contribution to each voxel is calculated by a clustering algorithm (Gevers et al., 2012). Most commonly used, the κ -mean clustering algorithm partitions the acquired perfusion maps into multiple territories by grouping voxels with similar inversion properties over all the vessel encoded images. This clustering approach works for any number of encoding steps. Identifying the individual contributions from multiple vessels in regions that are perfused by multiple sources is challenging. In order to identify the contributions of individual vessels to mixed perfusion

areas (e.g. watershed region), the κ - mean clustering can be supplemented with a linear analysis or be replaced by a Bayesian interference framework (Michael A. Chappell, Okell, Jezzard, & Woolrich, 2010; Hartkamp et al., 2014).

Ve-pcasl has also been adopted to quantify territorial perfusion in the absence of anatomical information (location of vessels within labeling plane). “Blind detection” of vessel location as well as territorial perfusion can be achieved by applying a large set encoding steps with random orientation and spacing (Eric C. Wong & Guo, 2012) or by using a Bayesian interference framework (Michael A. Chappell et al., 2010). More recent work has focused on optimizing ve-pcasl in terms of SNR and scanning time. Berry et al. (Berry, Jezzard, & Okell, 2015) proposed a framework to estimate SNR-optimized encoding steps based on Fourier Transformation which works for any number and assembly of vessels. A fast planning-free ve-pcasl approach was introduced by Zhang et al. (X. Zhang, Ghariq, Hartkamp, Webb, & Van Osch, 2016), which has shown to reduce the total acquisition time by interleaving blocks of label and control for different encoding steps.

As an alternative to ve-pcasl, Helle et al. (Helle et al., 2010) and Dai et al. (Dai, Robson, Shankaranarayanan, & Alsop, 2010) introduced the concept of super-selective pcasl to allow for the labeling of a single vessel. In this approach, the in-plane gradients are rotated within the label plane after each RF pulse, thereby creating a circular labeling area which can be placed freely on vessels in the neck and cranium (See the right panel of Figure 6). By changing the amplitude of the transverse gradients, the size of the label spot can be adjusted, providing precise measurements of individual perfusion territories. In comparison to ve-pcasl, super-selective PCASL does not require complicated post-processing to identify perfusion from an individual vessel. However, super-selective pcasl requires careful positioning of the label spot based on the subject’s anatomy.

Modeling the ASL signal

The ability to quantify physiological parameters, perfusion in particular, has motivated much of the development of ASL techniques. In the ASL literature, the single compartment model introduced by Buxton (Buxton et al., 1998) has generally been the *de facto* standard, and its solution for the continuous labeling case with post labeling delays is the recommended consensus implementation (Alsop et al., 2015) for routine use (The only difference between the two is that the former assumes that blood relaxes with the T1 of tissue when it enters the voxels, while the latter assumes that it continues to relax at the same rate as in the arteries). This model captures the behavior of the ASL signal in ideal continuous labeling experiments. However, it is also accepted that the behavior of the ASL signal is a bit more complex than that, and more complete models have also been proposed in order to capture the signal behavior (Parkes, 2005)(Zhou, Wilson, Ulatowski, Traystman, & van Zijl, 2001). Other types of ASL acquisitions, such as Look-Locker (Brookes, Morris, Gowland, & Francis, 2007)(Capron, Troalen, Cozzone, Bernard, & Kober, 2013; Noguchi et al., 2012) or fingerprinting acquisitions (Su et al., 2016; Wright, 2014) have also used modified versions of the model to account for these advanced acquisition techniques. As we will soon discuss, research has been focused on one and two compartment models, as well as the label dispersion in the arteries while in transit (M. a. Chappell et al., 2013). Additional factors like

the permeability of the vessels has also been explored (Ewing et al., 2006; St. Lawrence, Owen, & Wang, 2012; J. Wang, Fernández-Seara, Wang, & St Lawrence, 2007a).

Originally, the ASL signal was modeled by modification of the Bloch equations to include the inflow and outflow of blood magnetization (Detre et al., 1992; Williams et al., 1992). In the single compartmental model, it is assumed that blood enters the voxel volume being imaged through an artery and the exchange of water from the artery to the tissue is comprehensive and instantaneous, i.e., assuming a well-mixed compartment at the imaging voxel.

Another (simpler and more popular) way of describing the ASL signal in a single compartment model is through the convolution of the arterial magnetization function with a product of the “residue” (also referred to as “retention”) function $r(t)$, and a magnetization relaxation function $m(t)$ (Buxton et al., 1998; E C Wong et al., 1998).

The principal problem in using a single compartment model to describe the ASL signal is that the well-mixed compartment assumption does not hold very well in practice (see figure 8). The underlying assumption of instantaneous exchange of vascular water with tissue implies that that water in the voxel will relax with the $T1$ of tissue during the entirety of the ASL experiment, when in fact a portion of the blood relaxes with the $T1$ of blood before entering the tissue itself. This results in lower overall relaxation rates of labeled water in reality, because the $T1$ of water in blood is longer than $T1$ of water in tissue. Another aspect that leads to error is the assumption that all the blood in the artery is exchanged with the tissue in the voxel, whereas actually, a portion of the arriving blood passes through the voxel without exchanging water with the tissue.

The two-compartment model (see Figure 7) corrects for these effects by introduction of an additional compartment inside the voxel, where the blood enters from the artery. Exchange of water from this blood compartment into the tissue compartment occurs through the membrane separating the tissue and blood compartment, which is considered to be semipermeable. When this exchange is allowed, it is expressed with the help of the permeability-surface area (PS) product (Parkes, 2005)(Ewing, Cao, & Fenstermacher, 2001; St. Lawrence et al., 2012; J. Wang, Fernández-Seara, Wang, & St Lawrence, 2007b). When the assumption is that there is no exchange of labeled water between the blood and the tissue compartment, the permeability surface area product becomes unnecessary. Instead, it is assumed that the arterial input to the voxel branches into two components, a component that feeds blood into the tissue compartment and is absorbed in entirety, and a non-permeable pass-through arterial component, where there is no interaction with the tissue compartment.

In recent work for the purposes of ASL fingerprinting, Su et al. modified the Bloch equations for the two-compartmental model (see Figure 7) in order to capture the effects of arterial water flowing through a voxel without exchanging into the extravascular space (Su et al., 2016).

There has been a significant effort to include the effects of the dispersion of the blood particles as they travel from the labeling location to the imaging voxel. The arterial input function (AIF) describes the concentration of the label arriving at the tissue voxel as a

function of time. The ideal AIF for CASL would be a delayed box car shape reflecting the labeling scheme- indicating that the labeled bolus arrives at the imaging voxel identically to the manner in which it was labeled in the labeling plane. Early ASL work only accounted for the T1 relaxation of the arterial label and the transit time of the label from the labeling plane to the imaging slice (also referred to as “bolus arrival time”). However, such a formulation is inaccurate because in reality, deviations from the ideal situation above arise due to the labeled spins arriving at the imaging voxel at different speeds. In early work, Lewis and Hrabec (Hrabec & Lewis, 2004) included a Gaussian shaped dispersion kernel to capture this effect. Gallichan et al. introduced another dispersion model capturing the effects of laminar flow velocity profiles into the arrival time (Gallichan & Jezzard, 2008). However, more recent work from Chappell et al. demonstrated that a Gamma-Variate function was a better fit to the dispersion observed in the arterial input function (M. a. Chappell et al., 2013).

Physiological Noise Correction

The SNR of ASL images is intrinsically low, and a major contributor to the noise in ASL is signal fluctuations arising from cardiac pulsation and respiratory movements. Some recent improvements in SNR and stability of the ASL signal have been achieved by correcting the ASL time series for physiological noise. Methods used for physiological noise correction in ASL are often extended from those used in other fMRI methods. One such popular method is RETROICOR (Glover, I, & Ess, 2000) which uses low-order Fourier series to model the physiological noise component. This approach requires measurement of the physiological signals externally and removing them from an image time series through linear regression. This method was extended for ASL by Restom et al. (Restom, Behzadi, & Liu, 2006). The efficacy of the noise correction using this process depends on certain assumptions made in the modeling the noise, particularly regarding how the noise affects the control image compared to the tag image.

The CompCor method improves upon the RETROICOR procedure in that it does not require external recording (Behzadi, Restom, Liau, & Liu, 2007). This approach uses anatomical data in combination with variance maps of the ASL time course to identify white matter and cerebrospinal fluid. Oscillations in the perfusion signal of those regions are assumed to be dominated by physiological noise, rather than neuronal activation, which is assumed to be confined to the grey matter. Then a Principal Component Analysis (PCA) from time series extracted from the white matter and the CSF regions yields time course fluctuations due to cardiac and respiratory fluctuations. The largest components can be regressed from the ASL time course, or used in tandem with a general linear model as nuisance variables.

Partial Volume Correction

Partial Volume Effects in ASL arise due to the limited resolution of the acquired images. Usually, every voxel being imaged is a combination of white matter, gray matter and cerebrospinal fluid and, as a result, the effective ASL signal is a weighted average of signals from the different components in the voxel. Another cause of partial volume effects is that MRI acquisition schemes have an inherent point spread function that translates into a blurring in the image. Due to partial volume effects, the value of flow is often

underestimated, in addition to blurring the boundaries between tissue types. In order to alleviate these problems, several Partial Volume Correction (PVC) techniques have been developed.

One of the most prominent PVC techniques is the use of a linear regression method (Bruening, Dharssi, Lazar, Marshall, & Asllani, 2015) This technique involves estimating the unknown components in the expression for fractional ASL signal change:

$$\frac{\Delta M}{M_C} = \frac{(P_{GM}\Delta M_{GM}) + (P_{WM}\Delta M_{WM})}{(P_{GM}M_{GM}) + (P_{WM}M_{WM}) + (P_{CSF}M_{CSF})} \quad [2]$$

namely M_i - the difference between the control and label magnetization, with i denoting the tissue type, (GM for gray matter, WM for white matter, and CSF for cerebrospinal fluid) and M_i - the control magnetization for tissue type i . Other known factors are the prior probabilities for tissue type i in the imaging voxel, given by P_i , and the measured control magnetization, given by M_C . The estimation is done under the assumption that the perfusion level, and therefore the ASL signal, are constant over a small region (usually a 3×3 or 5×5 kernel) around the imaging voxel. Thus, one can construct a set of overdetermined linear equations for the signals in this region, and then solve for the unknown parameters using linear regression. However, this assumption of constancy causes an inherent blurring of the images corrected through this method. Attempts at removing this effect of blurring or overall smoothing have been made (Liang, Connelly, & Calamante, 2013) using modified least trimmed squares by removing outliers (in terms of residuals with respect to the kernel's central voxel) in the regression analysis of a region.

Another prominent method for PVC is the "Bayesian Inference for Arterial Spin Labelling" (BASIL) (M.A. Chappell, Groves, Whitcher, & Woolrich, 2009) method. This iterative method computes corrected perfusion values with a probabilistic non-linear least squares approach. Briefly, a Bayesian inference framework is used to calculate the posterior probability of the quantified parameters given the data, with the help of a likelihood term and an adaptive spatial smoothness prior for perfusion. More details about this are available to the reader in (M.A. Chappell et al., 2009; M. A. Chappell et al., 2011).

The necessary tissue type probability maps can be extracted from T1 weighted images and canonical templates. However, other methods like (Petr, Schramm, Hofheinz, Langner, & Van Den Hoff, 2013) aim at improving PVC by providing more consistent tissue probability maps (in terms of distortion and PSF) by using Look-Locker EPI for the generation of these maps, instead of using segmented high-resolution T1-weighted images. Bruening et al also presented an improved PVC method which uses high-dimensional structural space information (thereby extending the kernel into three dimensions) to combat the effects of signal mixing due to the composition of the voxel (Bruening et al., 2015).

Beyond perfusion: ASL and other physiological parameters

Among the most exciting new applications of ASL based techniques, their application to measure additional physiological parameters beyond perfusion, sometimes by modifications to the ASL acquisition scheme, sometimes by coupling the ASL measurement with other schemes.

By simply adapting the timing of the labeling scheme, for example, one can obtain quantitative images of the arterial blood volume. This is the case of the AVAST (Arterial Volume by Arterial Spin Tagging) technique (Jahanian, Peltier, Noll, & Garcia, 2015) in which the labeling time of a continuous labeling experiment is chosen to approximately match the bolus arrival time of the blood (i.e., the time it takes for the labeled spins to reach the voxel's tissue after they are labeled). Since the labeled spins have not entered the tissue yet, the observed ASL signal (i.e., subtraction of the control and labeled images) is dominated by the arterial blood, which yields an arterial blood volume weighted image. Further, if the sequence TR is reduced to match the bolus arrival time, which requires a small reduction in labeling time, then the label concentration in the extravascular space in both the control and labeled images is the same. In that case, the extravascular contribution to the ASL signal is removed by the pairwise subtraction process and the resulting image reflects only the arterial blood volume, without contamination by perfusion. Arterial blood volume is very sensitive to neuronal activation and can yield very high contrast to noise ratios in fMRI, as much of the BOLD effect is controlled by arterial vasodilation in the order to 30% (A.L. Vazquez, Lee, Hernandez-Garcia, & Noll, 2006; Alberto L Vazquez, Fukuda, Tasker, Masamoto, & Kim, 2010).

The VASO (Vascular Space Occupancy) technique also yields blood volume measurements by nulling out the contribution of the blood through the use of inversion pulses – much like the FLAIR technique. In its original implementation, it required the injection of a contrast agent like Gd-DTPA, which does not cross the blood brain barrier (Lu et al., 2005). In latter development, this need was overcome by the iVASO technique (Inflow-Based Vascular Space Occupancy), which uses combinations of selective and non-selective labeling pulses, much like pulsed ASL techniques (Hua et al., 2011;). Further progress along those lines has been made by combining labeling pulses with the sensitivity of multi-phase SSFP to inflowing blood. This technique results in high SNR, quantitative images of arterial blood volume, and could also be adapted to fMRI experiments (Yan, Li, Kilroy, Wehrli, & Wang, 2012).

Given that arterial spin labeling techniques can be used to isolate the blood's MR signal and that T_2 and T_2^* relaxation rates are sensitive to the blood's oxygenation level, techniques like TRUST (T2-Relaxation-Under-Spin-Tagging), can yield blood oxygenation (Y_v). In a nutshell, TRUST collects several ASL images with different effective echo time, and uses those to calculate the T_2 relaxation time of the ASL subtraction signal, as depicted in figure 9 (Liu et al., 2016; Lu & Ge, 2008; Lu, Zhao, Ge, & Lewis-Amezcuca, 2008; Xu, Ge, & Lu, 2009). This technique has some interesting features. The first one is that, in order to isolate the venous blood, the labeling pulse consists of a single, slab-selective, inversion pulse, applied downstream from the imaging slice (not upstream, as the regular ASL experiments),

such that the returning venous blood carries the label. The second interesting feature is that the T2 weighting of the signal is generated by a T2 preparation pulse train applied immediately before the image acquisition. This train of pulses consists of a 90 degree pulse followed by a train of 180 degree pulses that flip the magnetization in the transverse plane multiple times, while T2 contrast develops, and finally a -90 degree pulse to return the magnetization to the z-axis. The signs of the 180 degree pulses follows an MLEV pattern, in order to compensate for imperfections of the B1 field (Coolen et al., 2014). The T2 weighted images of the venous blood can then be used to compute the T2 relaxation rate. Finally, T2 can be readily translated into oxygenation level by previous T2-oxygenation calibration data obtained in vitro.

The QUIXOTIC technique yields similar information by isolating the post capillary venous blood through a clever combination of velocity selective saturation pulses and blood nulling inversion pulses. It offers the ability to collect venous blood oxygenation maps in grey matter regions (not just in the major venous watersheds). In the proposed implementation, the authors demonstrated that one can use this information in conjunction with ASL perfusion maps in order to calculate maps of the oxygen extraction fraction (OEF) and the metabolic rate of oxygen in the brain (CMRO₂) in addition to the venous oxygenation (Bolar, Rosen, Sorensen, & Adalsteinsson, 2011).

Another interesting physiological parameter that can be estimated with the help of arterial spin labeling is arterial transit time (ATT) or Bolus Arrival Time (BAT). BAT characterizes the time it takes the labeled blood to travel from the label plane in the neck to the tissue voxel in the brain (see figures 7 and 8).

It has been shown that BAT can vary significantly across different regions of the brain. One source of BAT variation is the difference in velocity between feeding arteries. For example, the velocity in the vertebral arteries is generally lower than in the carotid arteries. Another cause of transit delay is a longer travel distance, which for example occurs in the presence of collateral pathways. These non-uniformities in label transport can lead to significant errors in the quantification of perfusion signal. Commonly used quantification models (section: Single compartment and two compartment models) rely on a constant BAT across brain tissue. In order to make the quantification less sensitive to differences in BAT, typically a long post-labeling delay (PLD) is chosen ($PLD \gg BAT_{max}$) to guarantee that the label made it into the tissue and eliminate the contribution from the arterial compartment (Alsop & Detre, 1996). However, a long PLD leads to more label decay and therefore less SNR.

Variations in BAT are further amplified in the presence of disease. ASL perfusion images of patients with cerebrovascular disease often reveal regions of hypoperfusion. However, it is difficult to assess whether a decrease in label signal in a brain region is caused by a reduction in flow to this region or by a longer transit time. Prolonged BAT can therefore result in an underestimation of perfusion. BAT maps provide supplementary clinical information, which helps to interpret perfusion images and identify collateral pathways.

In order to acquire BAT maps, typically multiple ASL perfusion images are acquired, each with a different PLD. By tracking the perfusion signal over time, we can measure the label

uptake curve on a voxel-by-voxel basis. Based on the reconstructed label uptake curve, BAT can be estimated by finding the steepest rise in label uptake (Teeuwisse, Schmid, Ghariq, Veer, & Van Osch, 2014). However, this approach can lead to errors in the case of low temporal resolution or increased noise in the images. As an alternative, a single compartment model can be fitted to the uptake curve. Typically, 5–7 PLDs are necessary to reconstruct the label uptake curve sufficiently. The most straightforward approach is to acquire images with multiple PLDs consecutively. Assuming that a single ASL image acquisition takes about 3min, this would result in a total acquisition time of approximately 15–20 minutes, making it unfeasible for clinical use. Hence, research in this field has primarily focused on developing more efficient schemes to increase the acquisition speed.

One example is the application of a look-locker (LL) scheme, which has shown to increase the temporal resolution of multi-PLD acquisition (Y. Chen, Wang, & Detre, 2012). The LL scheme is based on multiple image acquisitions, immediately following the label pulse (Figure 10). Since each acquisition represents an increasing PLD, the gap before the next labeling period (TR) can be used efficiently. However, the LL scheme requires a low flip angle in order to acquire multiple images. While this improves the temporal resolution of the measurement, it results in a lower SNR compared to standard (single) acquisition schemes. This is especially true for the later portion of the curve, since the label will already have experienced multiple readout pulses.

As an alternative, time-encoded pcasl (te-pcasl) has been introduced to overcome low SNR and to acquire multiple PLDs in a single scan (Dai, Shankaranarayanan, & Alsop, 2013; Teeuwisse et al., 2014; Wells, Lythgoe, Gadian, Ordidge, & Thomas, 2010). Based on a Hadamard encoding scheme, te-pcasl splits up the pulse train in small blocks of labeling and control pulses (see Figure 11). In a post-processing step, the resulting perfusion image for a specific PLD can be calculated through a combination of all image acquisitions so that only one PLD remains whereas contributions from all other PLDs cancel out. In the example shown in Figure 11, the subtraction image for PLD 3 can be calculated as following:

$$\Delta M_{\text{PLD}3} = \text{Image 1} - \text{Image 2} + \text{Image 3} - \text{Image 4} - \text{Image 5} + \text{Image 6} - \text{Image 7} + \text{Image 8} \quad [3]$$

This approach has two major advantages. First, the combination of all acquisitions results in images with a high number of averages, which increases the SNR. Second, by using the entire time gap between the start of the pulse train and the image acquisition for blocks of label and control pulses, the entire scan can be performed in a fraction of the original scanning time for a sequential acquisition of PLDs. However, this approach also has a downside. The occurrence of artifacts, such as motion, will be carried through all images since each image is a combination of all acquisitions. More recently, It has been shown that the sensitivity to motion artefacts of te-pcasl can be reduced by replacing the Hadamard matrix with a Welsh-ordered Hadamard matrix (Federico von Samson-Himmelstjerna, Madai, Sobesky, & Guenther, 2016) or by using a Bayesian decoding scheme (F von Samson-Himmelstjerna, Chappell, Sobesky, & Günther, 2015).

ASL Fingerprinting

Magnetic Resonance Fingerprinting (MRF), originally proposed as a quantitative relaxometry method robust to artefacts (Ma et al., 2013) has been recently proposed as an alternative for estimating multiple physiological parameters related to blood flow and perfusion in the brain from a single time series (Su et al., 2016; Wright, 2014). Traditionally, acquiring these additional parameters typically requires extra scans, which renders the entire process time consuming and makes it clinically impractical. MRF tries to overcome this issue by matching an observed time-series of images to a dictionary composed of unique ASL signals. Their uniqueness is ensured by a (pseudo-) randomization of the acquisition parameters, e.g., label duration, TR, post labeling delay ...etc. The dictionary is generated by a signal model with multiple combinations of tissue parameters as its input, e.g., perfusion, blood volume, T1 ...etc. For each combination, a modified Bloch-equation simulation is performed based on a one- or two-compartment model (as described above), and the resultant time-series (see Figure 12) creates a single entry in the dictionary. The final step is to match each voxel's time series to the closest entry in the dictionary. The process of matching essentially mimics a Maximum Likelihood approach to estimate a set of parameters given an observation. Once the match is found, the tissue parameters used to generate the best match in the dictionary are assigned to that voxel. This process is repeated over all voxels in the imaging volume to obtain relevant parameter maps of the brain. As a result, fingerprinting can bypass difficulties in estimation caused by presence of artifacts, such as noise, off-resonance, movement or even undersampling.

ASL fingerprinting is still an active area of development. Current challenges include excessive amounts of storage space for the dictionary, as well as unacceptably long computational time to generate dictionaries and search for the best match. Despite this computational inefficiency, development of fingerprinting methods is exciting because they can be potentially robust to artefacts, while yielding multiple quantitative measurements from a single scan.

Resting State Functional Connectivity

Collecting a BOLD weighted time series without a specific activation paradigm or model is well known to reveal correlations in the activity among different brain areas (resting state functional connectivity rsfMRI). The spontaneous, correlated fluctuations used to identify networks using rsfMRI are typically slow, in the range below 0.1 Hz (Biswal, Kylen, & Hyde, 1997; Greicius, Krasnow, Reiss, & Menon, 2003). As can be expected, these fluctuations are also reflected in perfusion and several groups have demonstrated that ASL sequences can capture them and also reveal functionally connected networks similar to the ones found in BOLD imaging. Global correlations must be taken into account, as the observed ASL signal in the whole brain will fluctuate with respiration, cardiac pulsatility and any fluctuations in labeling efficiency. Despite these challenges, ASL still reveals functional networks, as first shown by Biswal et al in 1997 (Biswal et al., 1997) and further explored by others (Chuang et al., 2008; De Luca, Beckmann, De Stefano, Matthews, & Smith, 2006). BOLD weighted rsfMRI is more sensitive, offers higher temporal resolution and is simpler to implement, but ASL offers quantification as a very attractive feature. While

it is more common to perform separate ASL and BOLD connectivity scans, examples of ASL based rsfMRI include work by Loggia et al (Loggia et al., 2013), who examined changes in the default network related to chronic clinical pain. As the field of functional neuroimaging becomes increasingly quantitative, we can expect to see a rising trend in the use of ASL based functional connectivity imaging. An ambitious approach is to conduct interleaved ASL and BOLD time series measurements as the technique proposed by Schmitthorst et al (Schmitthorst et al., 2014). However, the more prevalent trend is to carry out BOLD weighted rsfMRI studies accompanied by ASL measurements of resting perfusion as a measure of baseline activity or to account for the vascular effects of drugs, as in the case of the study by Li et al. (Li & Zhang, 2017)

Applications

Over the first ten years since the publication of the first seminal papers, most of the research was focused on technical development, and the technique was not widely embraced by the larger imaging community. Many variants of the technique were developed trying to overcome serious challenges in SNR and resolution. For a long time, there was no clear standard implementation and it was rarely available from MRI vendors. ASL seemed like a “promising technique” under development, but only a few sites had the technical capability to use ASL in the clinic or as a research tool to investigate biological questions. In the last five to ten years, however, with the advent of improved labeling schemes, fast parallel imaging, background suppression and denoising techniques, ASL is rapidly gaining popularity in the clinic and in biomedical research. Most MRI vendor now have a standard implementation of the PCASL technique available for the new generation scanners.

Perfusion of blood through an organ is a powerful biomarker of its health and activity. As one could expect, the ability to image perfusion (dynamically, if necessary) without tracers or other invasive techniques has found many applications. In this section, we would like to survey a few recent applications of ASL, to illustrate the potential uses of the ASL technique, paying particular attention to neuroimaging applications.

To begin, much of the development of ASL techniques has been motivated by neurodegenerative and stroke research. Some of the earliest applications were centered on vascular disease, particularly stroke (Bokkers et al., 2012; Chalela et al., 2000; D. J. J. Wang et al., 2012; Zaharchuk, El Mogy, Fischbein, & Albers, 2012). For a thorough review of clinical neuroimaging applications of ASL, please see (Haller et al., 2016). More recently, the connection between vascular health and neurodegenerative disorders has become increasingly clear and has motivated many perfusion imaging studies in Alzheimer’s (Alsop, Detre, & Grossman, 2000; Benedictus et al., 2016; De La Torre, 2004; Iadecola, 2004) (Iturria-Medina et al., 2016) and Parkinson’s (Fernandez-Seara et al., 2012) diseases. In the case of Alzheimer’s disease, COST (the European Cooperation in Science and Technology) has been pursuing and funding an initiative to develop ASL as a tool to investigate and diagnose Alzheimers and other forms of dementia (<http://aslindementia.org>).

In this regard cognitive decline is strongly associated with hypoperfusion, which can also be a predictor of conversion from mild cognitive impairment to full blown dementia (Chao et

al., 2010; Wierenga, Hays, & Zlata, 2014). Recent studies have shown that perfusion imaging can also be informative about the severity of Parkinson's disease and it can also yield insights about its etiology and mechanism (Lin et al., 2017; Syrimi et al., 2017; Yamashita et al., 2017).

Perfusion imaging can be a key tool to examine longitudinal changes in brain function following an intervention, such as transcranial magnetic stimulation, cognitive training, or pharmacological treatment, in part because of their statistical properties (Aguirre, Detre, Zarahn, & Alsop, 2002). ASL techniques are largely immune to scanner drifts and can be used to quantify physiological parameters. For example, a recent study by Buch et al. (Buch, Ye, & Haacke, 2016) on caffeine and acetazolamide challenges (well known vasoactive drugs) highlights the utility of ASL techniques to probe changes in brain function caused by pharmacological intervention within a scanning session. At the same time, ASL based FMRI experiments can yield insights on the effects of psychoactive drugs over the course of the treatment, as in the recent study by Liemburg et al. (Liemburg, van Es, Knegtering, & Aleman, 2017), which showed differential effects between two different schizophrenia treatment medications in terms of how these affected the brain's response to emotional stimuli. ASL has also been used to identify the networks affected by Gamma hydroxybutyrate (GHB) in a double-blind, randomized cross-over design trial (Bosch et al., 2017). As another example, a randomised, double-blind, crossover phase II study is underway to examine the use of Tadalafil as a treatment for small vessel disease (SVD) and vascular cognitive impairment (VCI) (Pauls et al., 2017).

One of the dominant application of ASL is in cognitive psychology research. Notably, a recent large study of older participants (>70 years old) showed a clear correlation between several measures of cognition and baseline CBF (Hsieh et al., 2017). As an example of a task based ASL FMRI study, Buschkuel et al investigated the effect of working memory training on brain function during an N-back task. In their study, they showed that the improvement in performance was accompanied by perfusion differences in the brain both at rest and during task performance in selected regions (Buschkuehl, Hernandez-Garcia, Jaeggi, Bernard, & Jonides, 2014).

Finally, although the focus of this article is primarily brain imaging, it should also be noted that ASL is being used for other organs with increasing frequency, particularly the kidney (Duhamel, Prevost, Girard, Callot, & Cozzone, 2014; Mora-Gutierrez et al., 2017; Zimmer et al., 2013). A recent validation was carried out recently comparing ASL to dynamic contrast enhancement methods in the kidney by Conlin et al (Conlin et al., 2017).

References

- Aguirre GK, Detre Ja, Zarahn E, Alsop DC. 2002; Experimental design and the relative sensitivity of BOLD and perfusion fMRI. *NeuroImage*. 15(3):488–500. DOI: 10.1006/nimg.2001.0990 [PubMed: 11848692]
- Alsop DC, Detre Ja. 1996; Reduced transit-time sensitivity in noninvasive magnetic resonance imaging of human cerebral blood flow. *J Cereb Blood Flow Metab*. 16(6):1236–1249. DOI: 10.1097/00004647-199611000-00019 [PubMed: 8898697]
- Alsop DC, Detre JA, Golay X, Günther M, Hendrikse J, Hernandez-Garcia L, ... Zaharchuk G. 2015; Recommended implementation of arterial spin-labeled Perfusion mri for clinical applications: A

- consensus of the ISMRM Perfusion Study group and the European consortium for ASL in dementia. *Magnetic Resonance in Medicine*. 73(1)doi: 10.1002/mrm.25197
- Alsop DC, Detre JA, Grossman M. 2000; Assessment of cerebral blood flow in Alzheimer's disease by spin-labeled magnetic resonance imaging. *Annals of Neurology*. 47(1):93–100. [PubMed: 10632106]
- Behzadi Y, Restom K, Liu J, Liu TT. 2007; A component based noise correction method (CompCor) for BOLD and perfusion based fMRI. *NeuroImage*. 37(1):90–101. DOI: 10.1016/j.neuroimage.2007.04.042 [PubMed: 17560126]
- Benedictus MR, Leeuwis AE, Binnewijzend MAA, Kuijter JPA, Scheltens P, Barkhof F, ... Prins ND. 2016; Lower cerebral blood flow is associated with faster cognitive decline in Alzheimer's disease. *European Radiology*. 27(3):1–7. DOI: 10.1007/s00330-016-4450-z
- Berry ESK, Jezzard P, Okell TW. 2015; An Optimized Encoding Scheme for Planning Vessel-Encoded Pseudocontinuous Arterial Spin Labeling. *Magnetic Resonance in Medicine*. 74(5):1248–1256. DOI: 10.1002/mrm.25508 [PubMed: 25351616]
- Biswal BB, Van Kylen J, Hyde JS. 1997; Simultaneous assessment of flow and BOLD signals in resting-state functional connectivity maps. *NMR in Biomedicine*. 10(45):165–170. [PubMed: 9430343]
- Blaimer M, Breuer F, Mueller M, Heidemann RM, Griswold Ma, Jakob PM. 2004; SMASH, SENSE, PILS, GRAPPA: how to choose the optimal method. *Topics in Magnetic Resonance Imaging: TMRI*. 15(4):223–236. DOI: 10.1097/01.rmr.0000136558.09801.dd [PubMed: 15548953]
- Bokkers RPH, Hernandez DA, Merino JG, Mirasol RV, van Osch MJ, Hendrikse J, ... Latour LL. 2012; Whole-brain arterial spin labeling perfusion MRI in patients with acute stroke. *Stroke*. 43(5):1290–1294. [PubMed: 22426319]
- Bolar DS, Rosen BR, Sorensen AG, Adalsteinsson E. 2011; QUantitative Imaging of eXtraction of oxygen and Tissue consumption (QUIXOTIC) using venular-targeted velocity-selective spin labeling. *Magnetic Resonance in Medicine*. 66(6):1550–1562. DOI: 10.1002/mrm.22946 [PubMed: 21674615]
- Bosch, OG; Esposito, F; Havranek, MM; Dornbierer, D; von, Rotz R; Staempfli, P; ... Seifritz, E. Gamma-Hydroxybutyrate Increases Resting State Limbic Perfusion and Body and Emotion Awareness in Humans. *Neuropsychopharmacology*. 2017.
- Brookes MJ, Morris PG, Gowland Pa, Francis ST. 2007; Noninvasive measurement of arterial cerebral blood volume using Look-Locker EPI and arterial spin labeling. *Magnetic Resonance in Medicine*. 58(1):41–54. DOI: 10.1002/mrm.21199 [PubMed: 17659615]
- Bruening, DE; Dharssi, S; Lazar, RM; Marshall, RS; Asllani, I. Improved partial volume correction method for detecting brain activation in disease using Arterial Spin Labeling (ASL) fMRI. 2015 37th Annual International Conference of the IEEE Engineering in Medicine and Biology Society (EMBC), C; 2015. 5441–5444.
- Buch, S; Ye, Y; Haacke, EM. Quantifying the changes in oxygen extraction fraction and cerebral activity caused by caffeine and acetazolamide. *Journal of Cerebral Blood Flow & Metabolism*. 2016. 0271678X16641129.
- Buschkuhl M, Hernandez-Garcia L, Jaeggi SM, Bernard JA, Jonides J. 2014; Neural effects of short-term training on working memory. *Cognitive, Affective & Behavioral Neuroscience*. 14:147–60. DOI: 10.3758/s13415-013-0244-9
- Buxton RB, Frank LR, Wong EC, Siewert B, Warach S, Edelman RR. 1998; A general kinetic model for quantitative perfusion imaging with arterial spin labeling. *Magnetic Resonance in Medicine: Official Journal of the Society of Magnetic Resonance in Medicine/Society of Magnetic Resonance in Medicine*. 40:383–396. DOI: 10.1002/mrm.1910400308
- Capron T, Troalen T, Cozzone PJ, Bernard M, Kober F. 2013; Cine-ASL: A steady-pulsed arterial spin labeling method for myocardial perfusion mapping in mice. Part II. Theoretical model and sensitivity optimization. *Magnetic Resonance in Medicine*. 70(5):1399–1408. DOI: 10.1002/mrm.24588 [PubMed: 23281063]
- Chalela JA, Alsop DC, Gonzalez-Atavales JB, Maldjian JA, Kasner SE, Detre JA. 2000; Magnetic resonance perfusion imaging in acute ischemic stroke using continuous arterial spin labeling. *Stroke*. 31(3):680–687. [PubMed: 10700504]

- Chao LL, Buckley ST, Kornak J, Schuff N, Madison C, Yaffe K, ... Weiner MW. 2010; ASL perfusion MRI predicts cognitive decline and conversion from MCI to dementia. *Alzheimer Disease and Associated Disorders*. 24(1):19. [PubMed: 20220321]
- Chappell MA, Groves AR, MacIntosh BJ, Donahue MJ, Jezzard P, Woolrich MW. 2011; Partial volume correction of multiple inversion time arterial spin labeling MRI data. *Magnetic Resonance in Medicine*. 65(4):1173–1183. DOI: 10.1002/mrm.22641 [PubMed: 21337417]
- Chappell MA, Groves AR, Whitcher B, Woolrich MW. 2009; Variational Bayesian Inference for a Nonlinear Forward Model. *IEEE Transactions on Signal Processing*. 57(1):223–236. DOI: 10.1109/TSP.2008.2005752
- Chappell MA, Okell TW, Jezzard P, Woolrich MW. 2010; A general framework for the analysis of vessel encoded arterial spin labeling for vascular territory mapping. *Magnetic Resonance in Medicine*. 64(5):1529–1539. DOI: 10.1002/mrm.22524 [PubMed: 20677231]
- Chappell, Ma; Woolrich, MW; Kazan, S; Jezzard, P; Payne, SJ; MacIntosh, BJ. 2013; Modeling dispersion in arterial spin labeling: Validation using dynamic angiographic measurements. *Magnetic Resonance in Medicine*. 69(2):563–570. DOI: 10.1002/mrm.24260 [PubMed: 22489046]
- Chen JJ, Wieckowska M, Meyer E, Pike GB. 2008; Cerebral blood flow measurement using fMRI and PET: A cross-validation study. *International Journal of Biomedical Imaging*. 2008:516359.doi: 10.1155/2008/516359 [PubMed: 18825270]
- Chen Y, Wang DJJ, Detre Ja. 2011; Test-retest reliability of arterial spin labeling with common labeling strategies. *Journal of Magnetic Resonance Imaging*. 33(4):940–949. DOI: 10.1002/jmri.22345 [PubMed: 21448961]
- Chen Y, Wang DJJ, Detre JA. 2012; Comparison of arterial transit times estimated using arterial spin labeling. *Magnetic Resonance Materials in Physics, Biology and Medicine*. 25(2):135–144. DOI: 10.1007/s10334-011-0276-5
- Chuang KH, van Gelderen P, Merkle H, Bodurka J, Ikonomidou VN, Koretsky AP, ... Talagala SL. 2008; Mapping resting-state functional connectivity using perfusion MRI. *NeuroImage*. 40(4):1595–1605. DOI: 10.1016/j.neuroimage.2008.01.006 [PubMed: 18314354]
- Conlin CC, Oesingmann N, Bolster B, Huang Y, Lee VS, Zhang JL. 2017; Renal plasma flow (RPF) measured with multiple-inversion-time arterial spin labeling (ASL) and tracer kinetic analysis: Validation against a dynamic contrast-enhancement method. *Magnetic Resonance Imaging*. 37:51–55. DOI: 10.1016/j.mri.2016.11.010 [PubMed: 27864008]
- Coolen BF, Simonis FFI, Geelen T, Moonen RPM, Arslan F, Paulis LEM, ... Strijkers GJ. 2014; Quantitative T2 mapping of the mouse heart by segmented MLEV phase-cycled T2 preparation. *Magnetic Resonance in Medicine*. 72(2):409–417. [PubMed: 24186703]
- Dai W, Garcia D, De Bazelaire C, Alsop DC. 2008; Continuous flow-driven inversion for arterial spin labeling using pulsed radio frequency and gradient fields. *Magnetic Resonance in Medicine*. 60(6):1488–1497. DOI: 10.1002/mrm.21790 [PubMed: 19025913]
- Dai W, Robson PM, Shankaranarayanan A, Alsop DC. 2010; Modified pulsed continuous arterial spin labeling for labeling of a single artery. *Magnetic Resonance in Medicine*. 64(4):975–982. DOI: 10.1002/mrm.22363 [PubMed: 20665896]
- Dai W, Shankaranarayanan A, Alsop DC. 2013; Volumetric measurement of perfusion and arterial transit delay using hadamard encoded continuous arterial spin labeling. *Magnetic Resonance in Medicine*. 69(4):1014–1022. DOI: 10.1002/mrm.24335 [PubMed: 22618894]
- De La Torre JC. 2004; Is Alzheimer's disease a neurodegenerative or a vascular disorder? Data, dogma, and dialectics. *Lancet Neurology*. 3(3):184–190. DOI: 10.1016/S1474-4422(04)00683-0 [PubMed: 14980533]
- De Luca M, Beckmann CF, De Stefano N, Matthews PM, Smith SM. 2006; fMRI resting state networks define distinct modes of long-distance interactions in the human brain. *NeuroImage*. 29(4):1359–1367. [PubMed: 16260155]
- Deshmane A, Gulani V, Griswold MA, Seiberlich N. 2012; Parallel MR imaging. *Journal of Magnetic Resonance Imaging*. 36(1):55–72. DOI: 10.1002/jmri.23639 [PubMed: 22696125]
- Detre, Ja; Leigh, JS; Williams, DS; Koretsky, aP. 1992; Perfusion imaging. *Magnetic Resonance in Medicine: Official Journal of the Society of Magnetic Resonance in Medicine/Society of Magnetic Resonance in Medicine*. 23(1):37–45. DOI: 10.1002/mrm.1910230106

- Duhamel G, Prevost V, Girard OM, Callot V, Cozzone PJ. 2014; High-resolution mouse kidney perfusion imaging by pseudo-continuous arterial spin labeling at 11.75T. *Magnetic Resonance in Medicine*. 71:1186–1196. DOI: 10.1002/mrm.24740 [PubMed: 23568817]
- Ewing JR, Brown SL, Lu M, Panda S, Ding G, Knight Ra, ... Fenstermacher JD. 2006; Model selection in magnetic resonance imaging measurements of vascular permeability: Gadomer in a 9L model of rat cerebral tumor. *Journal of Cerebral Blood Flow and Metabolism: Official Journal of the International Society of Cerebral Blood Flow and Metabolism*. 26(3):310–320. DOI: 10.1038/sj.jcbfm.9600189
- Ewing JR, Cao Y, Fenstermacher J. 2001; Single-coil arterial spin-tagging for estimating cerebral blood flow as viewed from the capillary: Relative contributions of intra- and extravascular signal. *Magnetic Resonance in Medicine*. 46(3):465–475. DOI: 10.1002/mrm.1215 [PubMed: 11550237]
- Ewing JR, Cao Y, Knight Ra, Fenstermacher JD. 2005; Arterial spin labeling: Validity testing and comparison studies. *Journal of Magnetic Resonance Imaging*. 22(6):737–740. DOI: 10.1002/jmri.20451 [PubMed: 16261575]
- Fernandez-Seara, Ma; Mengual, E; Vidorreta, M; Aznarez-Sanado, M; Loayza, FR; Villagra, F; ... Pastor, Ma. 2012; Cortical hypoperfusion in Parkinson's disease assessed using arterial spin labeled perfusion MRI. *Neuroimage*. 59(3):2743–2750. DOI: 10.1016/j.neuroimage.2011.10.033 [PubMed: 22032942]
- Gallichan D, Jezzard P. 2008; Modeling the effects of dispersion and pulsatility of blood flow in pulsed arterial spin labeling. *Magnetic Resonance in Medicine*. 60(1):53–63. DOI: 10.1002/mrm.21654 [PubMed: 18581416]
- Gao Y, Goodnough CL, Erokwu BO, Farr GW, Darrah R, Lu L, ... Flask Ca. 2014; Arterial spin labeling-fast imaging with steady-state free precession (ASL-FISP): A rapid and quantitative perfusion technique for high-field MRI. *NMR in Biomedicine*. 27(8):996–1004. DOI: 10.1002/nbm.3143 [PubMed: 24891124]
- Garcia DM, Duhamel G, Alsop DC. 2005; Efficiency of inversion pulses for background suppressed arterial spin labeling. *Magnetic Resonance in Medicine*. 54(2):366–372. DOI: 10.1002/mrm.20556 [PubMed: 16032674]
- Gevers S, Bokkers RP, Hendrikse J, Majoie CB, Kies DA, Teeuwisse WM, ... Van Osch MJ. 2012; Robustness and reproducibility of flow territories defined by planning-free vessel- encoded pseudocontinuous arterial spin-labeling. *American Journal of Neuroradiology*. 33(2):21–25. DOI: 10.3174/ajnr.A2410
- Glover GARYH, ITIEIL, Ess DAR. 2000 Image-Based Method for Retrospective Correction of Physiological Motion Effects in fMRI: RETROICOR. 167Mar.:162–167.
- Greicius MD, Krasnow B, Reiss AL, Menon V. 2003; Functional connectivity in the resting brain: a network analysis of the default mode hypothesis. *Proceedings of the National Academy of Sciences of the United States of America*. 100(1):253–258. DOI: 10.1073/pnas.0135058100 [PubMed: 12506194]
- Guo, J; Meakin, Ja; Jezzard, P; Wong, EC. An optimized design to reduce eddy current sensitivity in velocity-selective arterial spin labeling using symmetric BIR-8 pulses. *Magnetic Resonance in Medicine*. 2014. n/a-n/a. JOUR.
- Haller S, Zaharchuk G, Thomas DL, Lovblad KO, Barkhof F, Golay X. 2016; Arterial Spin Labeling Perfusion of the Brain: Emerging Clinical Applications. *Radiology*. 281(2):337–356. DOI: 10.1148/radiol.2016150789 [PubMed: 27755938]
- Hartkamp NS, Helle M, Chappell MA, Okell TW, Hendrikse J, Bokkers RPH, Van Osch MJP. 2014; Validation of planning-free vessel-encoded pseudo-continuous arterial spin labeling MR imaging as territorial-ASL strategy by comparison to super-selective p-CASL MRI. *Magnetic Resonance in Medicine*. 71(6):2059–2070. DOI: 10.1002/mrm.24872 [PubMed: 23878062]
- Helle M, Norris DG, Rüfer S, Alfke K, Jansen O, Van Osch MJP. 2010; Superselective pseudocontinuous arterial spin labeling. *Magnetic Resonance in Medicine*. 64(3):777–786. DOI: 10.1002/mrm.22451 [PubMed: 20597127]
- Hrabe J, Lewis DP. 2004; Two analytical solutions for a model of pulsed arterial spin labeling with randomized blood arrival times. *Journal of Magnetic Resonance*. 167(1):49–55. DOI: 10.1016/j.jmr.2003.11.002 [PubMed: 14987598]

- Hshieh TT, Dai W, Cavallari M, Guttmann CR, Meier DS, Schmitt EM, ... Alsop DC. 2017; Cerebral blood flow MRI in the nondemented elderly is not predictive of post-operative delirium but is correlated with cognitive performance. *Journal of Cerebral Blood Flow & Metabolism*. 37(4): 1386–1397. DOI: 10.1177/0271678X16656014 [PubMed: 27401806]
- Hua J, Qin Q, Donahue MJ, Zhou J, Pekar JJ, Van Zijl PCM. 2011; Inflow-based vascular-space-occupancy (iVASO) MRI. *Magnetic Resonance in Medicine*. 66(1):40–56. DOI: 10.1002/mrm.22775 [PubMed: 21695719]
- Iadecola C. 2004; Neurovascular regulation in the normal brain and in Alzheimer's disease. *Nature Reviews. Neuroscience*. 5(5):347–360. DOI: 10.1038/nrn1387 [PubMed: 15100718]
- Iturria-Medina Y, Sotero RC, Toussaint PJ, Mateos-Pérez JM, Evans AC, Weiner MW, ... Furst AJ. 2016 Early role of vascular dysregulation on late-onset Alzheimer's disease based on multifactorial data-driven analysis. *Nature Communications*. 7May.doi: 10.1038/ncomms11934
- Jahanian H, Peltier S, Noll DC, Garcia LH. 2015; Arterial cerebral blood volume-weighted functional MRI using pseudocontinuous arterial spin tagging (AVAST). *Magnetic Resonance in Medicine*. 73(3)doi: 10.1002/mrm.25220
- Li CX, Zhang X. 2017; Effects of long-duration administration of 1% isoflurane on resting cerebral blood flow and default mode network in macaque monkeys. *Brain Connectivity*. 7(2):98–105. [PubMed: 28030956]
- Liang X, Connelly A, Calamante F. 2013; Improved partial volume correction for single inversion time arterial spin labeling data. *Magnetic Resonance in Medicine*. 69(2):531–537. DOI: 10.1002/mrm.24279 [PubMed: 22528959]
- Liemburg EJ, van Es F, Knegtering H, Aleman A. 2017 Effects of aripiprazole versus risperidone on brain activation during planning and social-emotional evaluation schizophrenia: A single-blind randomized exploratory study. *Progress in Neuro-Psychopharmacology and Biological Psychiatry*.
- Lin W-C, Chen P-C, Huang C-C, Tsai N-W, Chen H-L, Wang H-C, ... Lu C-H. 2017 Autonomic Function Impairment and Brain Perfusion deficit in Parkinson's Disease. *Frontiers in Neurology*. : 8. [PubMed: 28163694]
- Liu P, Dimitrov I, Andrews T, Crane DE, Dariotis JK, Desmond J, ... Lu H. 2016; Multisite evaluations of a T2-relaxation-under-spin-tagging (TRUST) MRI technique to measure brain oxygenation. *Magnetic Resonance in Medicine*. 75(2):680–687. DOI: 10.1002/mrm.25627 [PubMed: 25845468]
- Loggia ML, Kim J, Gollub RL, Vangel MG, Kirsch I, Kong J, ... Napadow V. 2013; Default mode network connectivity encodes clinical pain: An arterial spin labeling study. *Pain*. 154(1):24–33. DOI: 10.1016/j.pain.2012.07.029 [PubMed: 23111164]
- Lu H, Ge Y. 2008; Quantitative evaluation of oxygenation in venous vessels using T2-relaxation-under-spin-tagging MRI. *Magnetic Resonance in Medicine*. 60(2):357–363. DOI: 10.1002/mrm.21627 [PubMed: 18666116]
- Lu H, Law M, Johnson G, Ge Y, Van Zijl PCM, Helpert Ja. 2005; Novel approach to the measurement of absolute cerebral blood volume using vascular-space-occupancy magnetic resonance imaging. *Magnetic Resonance in Medicine*. 54(6):1403–1411. DOI: 10.1002/mrm.20705 [PubMed: 16254955]
- Lu H, Zhao C, Ge Y, Lewis-Amezcu K. 2008; Baseline blood oxygenation modulates response amplitude: Physiologic basis for intersubject variations in functional MRI signals. *Magnetic Resonance in Medicine*. 60(2):364–372. DOI: 10.1002/mrm.21686 [PubMed: 18666103]
- Ma D, Gulani V, Seiberlich N, Liu K, Sunshine JL, Duerk JL, Griswold Ma. 2013; Magnetic resonance fingerprinting. *Nature*. 495(7440):187–192. DOI: 10.1038/nature11971 [PubMed: 23486058]
- Meakin, Ja; Jezzard, P. 2013; An optimized velocity selective arterial spin labeling module with reduced eddy current sensitivity for improved perfusion quantification. *Magnetic Resonance in Medicine*. 69(3):832–838. DOI: 10.1002/mrm.24302 [PubMed: 22556043]
- Mora-Gutierrez, JM; Garcia-Fernandez, N; Slon, Roblero MF; Paramo, JA; Escalada, FJ; Wang, DJ; ... Ndez-Seara, MA. Arterial spin labeling MRI is able to detect early hemodynamic changes in diabetic nephropathy. *Journal of Magnetic Resonance Imaging*. 2017.
- Noguchi T, Yoshiura T, Hiwatashi A, Togao O, Yamashita K, Nagao E, Honda H. 2012; Arterial spin-labeling magnetic resonance imaging: The timing of regional maximal perfusion-related signal

- intensity revealed by a multiphase technique. *Japanese Journal of Radiology*. 30(2):137–145. DOI: 10.1007/s11604-011-0025-8 [PubMed: 22173560]
- Norris DG, Schwarzbauer C. 1999; Velocity selective radiofrequency pulse trains. *Journal of Magnetic Resonance (San Diego, Calif: 1997)*. 137:231–236. DOI: 10.1006/jmre.1998.1690
- Obara M, Togao O, Yoneyama M, Okuaki T, Shibukawa S, Honda H, Van Cauteren M. 2016; Acceleration-selective arterial spin labeling for intracranial MR angiography with improved visualization of cortical arteries and suppression of cortical veins. *Magnetic Resonance in Medicine*. 0:1–9. DOI: 10.1002/mrm.26275
- Parkes LM. 2005; Quantification of cerebral perfusion using arterial spin labeling: Two-compartment models. *Journal of Magnetic Resonance Imaging*. 22(6):732–736. DOI: 10.1002/jmri.20456 [PubMed: 16267854]
- Pauls MMH, Clarke N, Trippier S, Betteridge S, Howe FA, Khan U, ... Pereira AC. 2017; Perfusion by Arterial Spin labelling following Single dose Tadalafil In Small vessel disease (PASTIS): study protocol for a randomised controlled trial. *Trials*. 18(1):229. [PubMed: 28532471]
- Perthen JE, Bydder M, Restom K, Liu TT. 2008; SNR and functional sensitivity of BOLD and perfusion-based fMRI using arterial spin labeling with spiral SENSE at 3 T. *Magnetic Resonance Imaging*. 26(4):513–522. DOI: 10.1016/j.mri.2007.10.008 [PubMed: 18158226]
- Petr J, Schramm G, Hofheinz F, Langner J, Van Den Hoff J. 2013; Partial volume correction in arterial spin labeling using a Look-Locker sequence. *Magnetic Resonance in Medicine*. 70(6):1535–1543. DOI: 10.1002/mrm.24601 [PubMed: 23280559]
- Pruessmann KP, Weiger M, Scheidegger MB, Boesiger P. 1999; SENSE: Sensitivity encoding for fast MRI. *Magnetic Resonance in Medicine*. 42(5):952–962. DOI: 10.1002/(SICI)1522-2594(199911)42:5<952::AID-MRM16>3.0.CO;2-S [PubMed: 10542355]
- Qin, Q; Shin, T; Schär, M; Guo, H; Chen, H; Qiao, Y. Velocity-selective magnetization-prepared non-contrast-enhanced cerebral MR angiography at 3 tesla: Improved immunity to b0/b1 inhomogeneity. *Magnetic Resonance in Medicine*. 2015. 0, n/a-n/a.
- Qin Q, van Zijl PCM. 2016; Velocity-selective-inversion prepared arterial spin labeling. *Magnetic Resonance in Medicine*. 76(4):1136–1148. DOI: 10.1002/mrm.26010 [PubMed: 26507471]
- Restom K, Behzadi Y, Liu TT. 2006; Physiological noise reduction for arterial spin labeling functional MRI. *NeuroImage*. 31(3):1104–1115. DOI: 10.1016/j.neuroimage.2006.01.026 [PubMed: 16533609]
- Richter XV, Helle XM, Osch XMJP, Van Lindner XT, Gersing XAS, Tsantilas XP, ... Preibisch XC. 2017 ADULT BRAIN MR Imaging of Individual Perfusion Reorganization Using Superselective Pseudocontinuous Arterial Spin-Labeling in Patients with Complex Extracranial Steno-Occlusive Disease. :1–9.
- Schmid S, Ghariq E, Teeuwisse WM, Webb A, Van Osch MJP. 2014; Acceleration-selective arterial spin labeling. *Magnetic Resonance in Medicine*. 71:191–199. DOI: 10.1002/mrm.24650 [PubMed: 23483624]
- Schmid S, Heijtel DFR, Mutsaerts HJMM, Boellaard R, Lammertsma Aa, Nederveen AJ, Van Osch MJP. 2014; Comparison of velocity and acceleration selective arterial spin labeling with ¹⁵O H₂O positron emission tomography. 32(1):4056.doi: 10.1038/jcbfm.2015.42
- Schmithorst VJ, Hernandez-Garcia L, Vannest J, Rajagopal A, Lee G, Holland SK. 2014; Optimized simultaneous ASL and BOLD functional imaging of the whole brain. *Journal of Magnetic Resonance Imaging*. 39:1104–1117. DOI: 10.1002/jmri.24273 [PubMed: 24115454]
- St Lawrence KS, Frank Ja, Bandettini Pa, Ye FQ. 2005; Noise reduction in multi-slice arterial spin tagging imaging. *Magnetic Resonance in Medicine*. 53(3):735–738. DOI: 10.1002/mrm.20396 [PubMed: 15723412]
- St Lawrence KS, Owen D, Wang DJJ. 2012; A two-stage approach for measuring vascular water exchange and arterial transit time by diffusion-weighted perfusion MRI. *Magnetic Resonance in Medicine*. 67(5):1275–1284. DOI: 10.1002/mrm.23104 [PubMed: 21858870]
- Su P, Mao D, Liu P, Li Y, Pinho MC, Welch BG, Lu H. 2016 Multiparametric estimation of brain hemodynamics with MR fingerprinting ASL. *Magnetic Resonance in Medicine*. 0Nov.:1–12. DOI: 10.1002/mrm.26587

- Syrimi ZJ, Vojtisek L, Eliasova I, Viskova J, Svatkova A, Vanicek J, Rektorova I. 2017; Arterial spin labelling detects posterior cortical hypoperfusion in non-demented patients with Parkinson's disease. *Journal of Neural Transmission*. 124(5):551–557. [PubMed: 28271290]
- Teeuwisse WM, Schmid S, Ghariq E, Veer IM, Van Osch MJP. 2014; Time-encoded pseudocontinuous arterial spin labeling: Basic properties and timing strategies for human applications. *Magnetic Resonance in Medicine*. 72(6):1712–1722. DOI: 10.1002/mrm.25083 [PubMed: 24395462]
- Van Gelderen P, De Zwart Ja, Duyn JH. 2008; Pitfalls of MRI measurement of white matter perfusion based on arterial spin labeling. *Magnetic Resonance in Medicine*. 59(4):788–795. DOI: 10.1002/mrm.21515 [PubMed: 18383289]
- Van Osch MJP, Teeuwisse WM, Van Walderveen Maa, Hendrikse J, Kies Da, Van Buchem Ma. 2009; Can arterial spin labeling detect white matter perfusion signal? *Magnetic Resonance in Medicine*. 62(1):165–173. DOI: 10.1002/mrm.22002 [PubMed: 19365865]
- Vazquez AL, Fukuda M, Tasker ML, Masamoto K, Kim SG. 2010; Changes in cerebral arterial, tissue and venous oxygenation with evoked neural stimulation: implications for hemoglobin-based functional neuroimaging. *Journal of Cerebral Blood Flow and Metabolism: Official Journal of the International Society of Cerebral Blood Flow and Metabolism*. 30(2):428–439. DOI: 10.1038/jcbfm.2009.213
- Vazquez AL, Lee GR, Hernandez-Garcia L, Noll DC. 2006; Application of selective saturation to image the dynamics of arterial blood flow during brain activation using magnetic resonance imaging. *Magnetic Resonance in Medicine*. 55(4)doi: 10.1002/mrm.20813
- von Samson-Himmelstjerna F, Chappell MA, Sobesky J, Günther M. 2015; Subtraction free arterial spin labeling: A new Bayesian-inference based approach for gaining perfusion data from time encoded data. *Proceedings of the International Society for Magnetic Resonance in Medicine (ISMRM)*. : 275.
- von Samson-Himmelstjerna F, Madai VI, Sobesky J, Guenther M. 2016; Walsh-ordered hadamard time-encoded pseudocontinuous ASL (WH pCASL). *Magnetic Resonance in Medicine*. 76(6): 1814–1824. DOI: 10.1002/mrm.26078 [PubMed: 26714671]
- Wang DJJ, Alger JR, Qiao JX, Hao Q, Hou S, Fiaz R, ... Salamon N. 2012; The value of arterial spin-labeled perfusion imaging in acute ischemic stroke. *Stroke*. 43(4):1018–1024. [PubMed: 22328551]
- Wang J, Fernández-Seara Ma, Wang S, St Lawrence KS. 2007a; When perfusion meets diffusion: in vivo measurement of water permeability in human brain. *Journal of Cerebral Blood Flow and Metabolism: Official Journal of the International Society of Cerebral Blood Flow and Metabolism*. 27(4):839–849. DOI: 10.1038/sj.jcbfm.9600398
- Wang J, Fernández-Seara Ma, Wang S, St Lawrence KS. 2007b; When perfusion meets diffusion: in vivo measurement of water permeability in human brain. *Journal of Cerebral Blood Flow and Metabolism: Official Journal of the International Society of Cerebral Blood Flow and Metabolism*. 27(4):839–849. DOI: 10.1038/sj.jcbfm.9600398
- Wells JA, Lythgoe MF, Gadian DG, Ordidge RJ, Thomas DL. 2010; In vivo Hadamard encoded Continuous arterial spin labeling (H-CASL). *Magnetic Resonance in Medicine*. 63(4):1111–1118. DOI: 10.1002/mrm.22266 [PubMed: 20373414]
- Wierenga CE, Hays CC, Zlatar ZZ. 2014; Cerebral blood flow measured by arterial spin labeling MRI as a preclinical marker of Alzheimer's disease. *Journal of Alzheimer's Disease*. 42(s4):S411–S419.
- Williams DS, Detre Ja, Leigh JS, Koretsky aP. 1992; Magnetic resonance imaging of perfusion using spin inversion of arterial water. *Proceedings of the National Academy of Sciences of the United States of America*. 89(1):212–216. DOI: 10.1073/pnas.89.9.4220e [PubMed: 1729691]
- Wolff SD, Balaban RS. 1989; Magnetization transfer contrast (MTC) and tissue water proton relaxation in vivo. *Magnetic Resonance in Medicine: Official Journal of the Society of Magnetic Resonance in Medicine/Society of Magnetic Resonance in Medicine*. 10(1):135–144. DOI: 10.1002/mrm.1910100113
- Wong EC. 2007; Vessel-encoded arterial spin-labeling using pseudocontinuous tagging. *Magnetic Resonance in Medicine*. 58(6):1086–1091. DOI: 10.1002/mrm.21293 [PubMed: 17969084]

- Wong EC, Buxton RB, Frank LR. 1998; A theoretical and experimental comparison of continuous and pulsed arterial spin labeling techniques for quantitative perfusion imaging. *Magnetic Resonance in Medicine: Official Journal of the Society of Magnetic Resonance in Medicine/Society of Magnetic Resonance in Medicine*. 40(3):348–355.
- Wong EC, Cronin M, Wu WC, Inglis B, Frank LR, Liu TT. 2006; Velocity-selective arterial spin labeling. *Magnetic Resonance in Medicine: Official Journal of the Society of Magnetic Resonance in Medicine/Society of Magnetic Resonance in Medicine*. 55(6):1334–1341. DOI: 10.1002/mrm.20906
- Wong EC, Guo J. 2012; Blind detection of vascular sources and territories using random vessel encoded arterial spin labeling. *Magnetic Resonance Materials in Physics, Biology and Medicine*. 25(2):95–101. DOI: 10.1007/s10334-011-0302-7
- Wright KL. 2014; Theoretical Framework for MR Fingerprinting with ASL: Simultaneous Quantification of CBF, Transit Time, and T1. *Isrmr*. 1:1.
- Wu WC, Wong EC. 2007; Feasibility of velocity selective arterial spin labeling in functional MRI. *Journal of Cerebral Blood Flow and Metabolism: Official Journal of the International Society of Cerebral Blood Flow and Metabolism*. 27(4):831–838. DOI: 10.1038/sj.jcbfm.9600386
- Xu F, Ge Y, Lu H. 2009; Noninvasive quantification of whole-brain cerebral metabolic rate of oxygen (CMRO₂) by MRI. *Magnetic Resonance in Medicine*. 62(1):141–148. DOI: 10.1002/mrm.21994 [PubMed: 19353674]
- Yamashita K, Hiwatashi A, Togao O, Kikuchi K, Yamaguchi H, Suzuki Y, ... Honda H. 2017; Cerebral blood flow laterality derived from arterial spin labeling as a biomarker for assessing the disease severity of parkinson's disease. *Journal of Magnetic Resonance Imaging*. 45(6):1821–1826. [PubMed: 27696565]
- Yan L, Li C, Kilroy E, Wehrli FW, Wang DJJ. 2012; Quantification of arterial cerebral blood volume using multiphase-balanced SSFP-based ASL. *Magnetic Resonance in Medicine*. 68(1):130–139. DOI: 10.1002/mrm.23218 [PubMed: 22127983]
- Ye FQ, Berman KF, Ellmore T, et al. 2000; H(2)(15)O PET validation of steady-state arterial spin tagging cerebral blood flow measurements in humans. *Magn Reson Med*. 44(3):450–6. [PubMed: 10975898]
- Ye FQ, Frank JA, Weinberger DR, McLaughlin AC. 2000; Noise reduction in 3D perfusion imaging by attenuating the static signal in arterial spin tagging (ASSIST). *Magnetic Resonance in Medicine*. 44(1):92–100. DOI: 10.1002/1522-2594(200007)44:1<92::AID-MRM14>3.0.CO;2-M [PubMed: 10893526]
- Zaharchuk G, El Mogy IS, Fischbein NJ, Albers GW. 2012; Comparison of arterial spin labeling and bolus perfusion-weighted imaging for detecting mismatch in acute stroke. *Stroke*. 43(7):1843–1848. [PubMed: 22539548]
- Zhang W, Silva aC, Williams DS, Koretsky aP. 1995; NMR measurement of perfusion using arterial spin labeling without saturation of macromolecular spins. *Magnetic Resonance in Medicine*. 33(3):370–376. DOI: 10.1002/mrm.1910330310 [PubMed: 7760704]
- Zhang X, Ghariq E, Hartkamp NS, Webb AG, Van Osch MJP. 2016; Fast cerebral flow territory mapping using vessel encoded dynamic arterial spin labeling (VE-DASL). *Magnetic Resonance in Medicine*. 75(5):2041–2049. DOI: 10.1002/mrm.25806 [PubMed: 26094586]
- Zhou J, Wilson DA, Ulatowski JA, Traystman RJ, van Zijl PCM. 2001; Two-Compartment Exchange Model for Perfusion Quantification Using Arterial Spin Tagging. *Journal of Cerebral Blood Flow & Metabolism*. 21(4):440–455. DOI: 10.1097/00004647-200104000-00013 [PubMed: 11323530]
- Zimmer F, Zöllner FG, Hoeger S, Klotz S, Tsagogiorgas C, Krämer BK, Schad LR. 2013; Quantitative Renal Perfusion Measurements in a Rat Model of Acute Kidney Injury at 3T: Testing Inter- and Intramethodical Significance of ASL and DCE-MRI. *PLoS ONE*. 8(1)doi: 10.1371/journal.pone.0053849

This is a review article regarding the recent advances made in the area of hemodynamic parameter imaging using ASL techniques.

After a brief overview of the technique's fundamentals, this article will review new trends and variants of ASL including different labeling schemes, vascular territory mapping and velocity selective ASL, as well as arterial blood volume imaging techniques.

This article will also review recent processing techniques to reduce partial volume effects and physiological noise.

Next, the article will examine how ASL techniques can be leveraged to calculate additional physiological parameters beyond perfusion and finally, it will review a few recent applications of ASL in the literature.

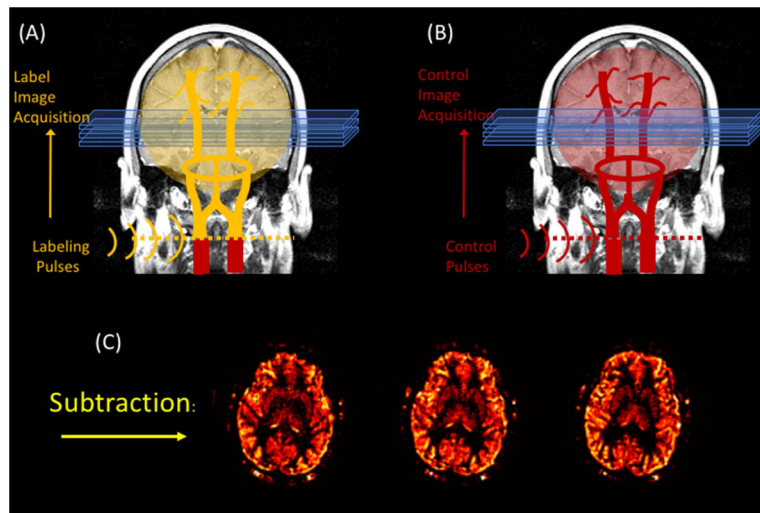


Figure 1. A basic pseudo-continuous ASL experiment. The arterial water is inverted as it crosses a plane through the neck prior to acquiring the “labeled” image. A second “control” image is acquired without the label. The subtraction of these two images yields a perfusion weighted image.

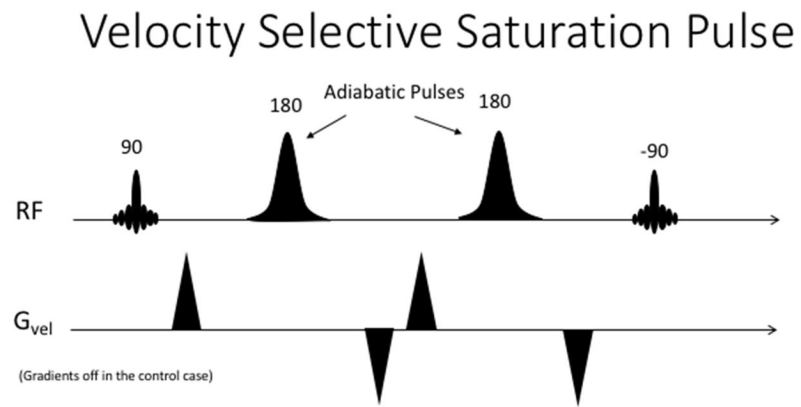


Figure 2.
A basic velocity selective labeling pulse train.

BIR-8 Velocity Selective Saturation Pulse

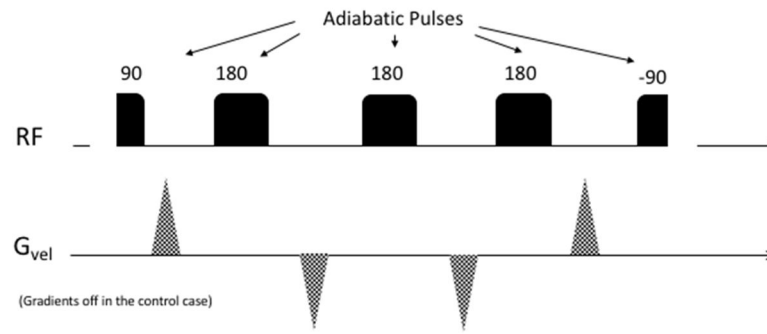


Figure 3. Velocity Selective Saturation pulses using a BIR-8 scheme in order to reduce eddy current artefacts. In the control case, the velocity selective gradients are turned off.

Velocity Selective Inversion Pulse

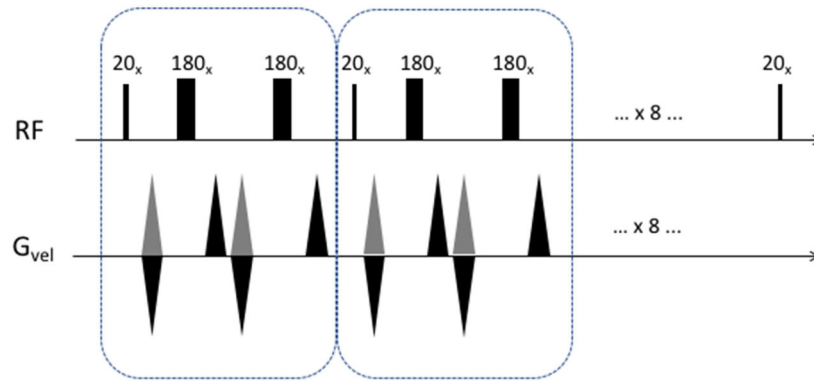


Figure 4.

Velocity Selective Inversion pulse described by Qin et al. A 180 degree hard pulse is broken into nine 20 degree segments. Additional 180's are interspersed to refocus off-resonance effects and correct for B1 inhomogeneity. These follow an MLEV phase pattern. In the control case, the velocity selective gradients are always positive (shown in grey).

Vessel Selective PCASL Train

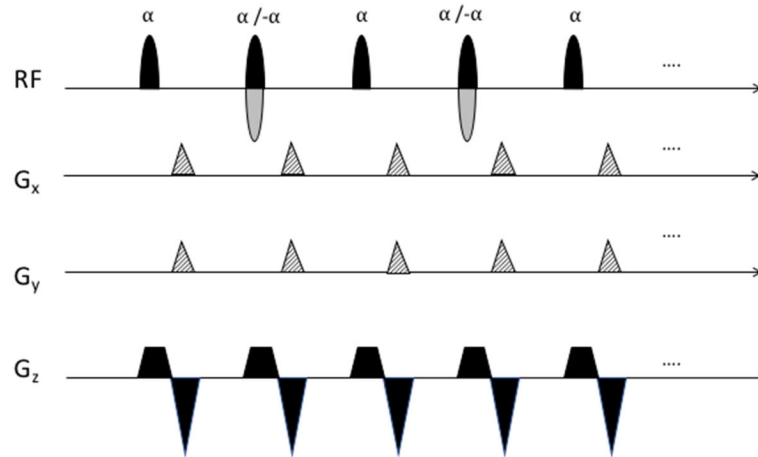


Figure 5.

A vessel selective pseudo-continuous labeling pulse train. G_x and G_y represent the additional in-plane gradients which allow to label individual vessels within the labeling plane. These gradients are played in the gap between RF pulses, typically at the same time as the rephaser of the slice selective gradient. In the control case, the sign of the RF pulses is alternated every other pulse (shown in grey).

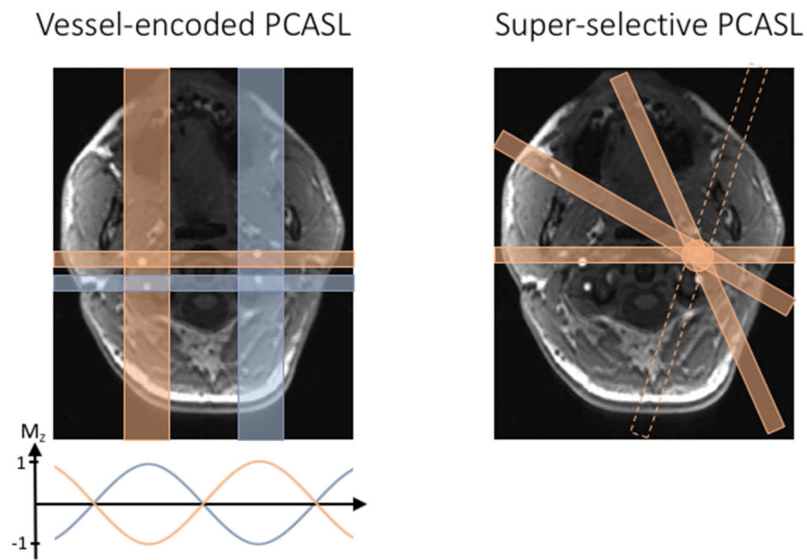


Figure 6. Vessel-selective labeling schemes. The left panel shows a vessel-encoded labeling pattern that labels specific groups of arteries. The in-plane gradients generate a linear phase variation along the gradient direction, resulting in an approximately sinusoidal inversion profile across the label plane. The individual perfusion territories are then calculated by either solving a set of linear equations or by using a clustering approach. The right panel shows a schematic of the super-selective labeling scheme, which can isolate individual arteries by rotating the “labeling band” during the pseudo continuous labeling train of pulses.

ASL Signal Models

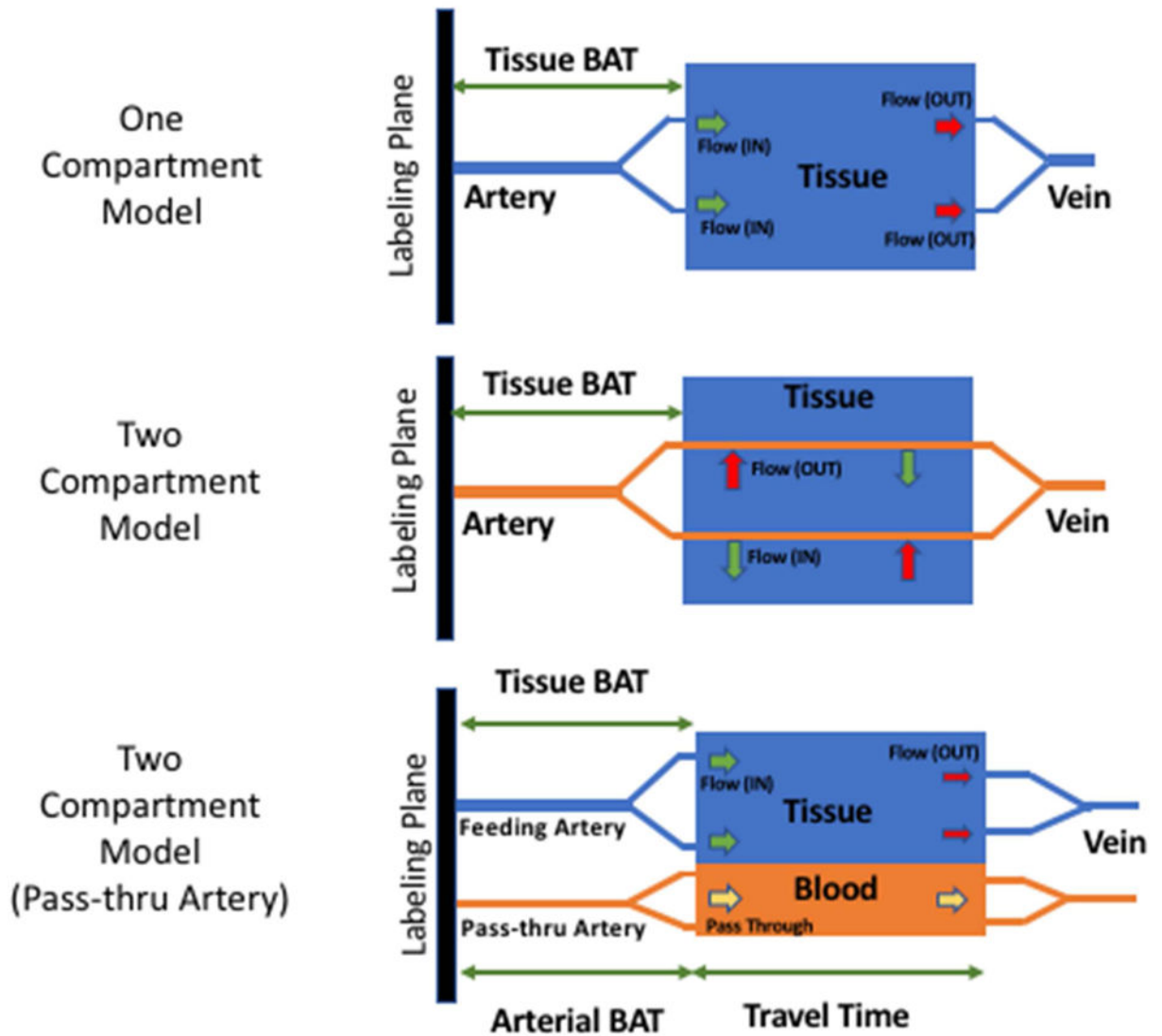


Figure 7. The ASL signal can be modeled by describing the concentration of label in the voxel using one compartment and two compartments. The two-compartment model has also been modified in order to capture flow-thru effects.

Modeling the ASL signal

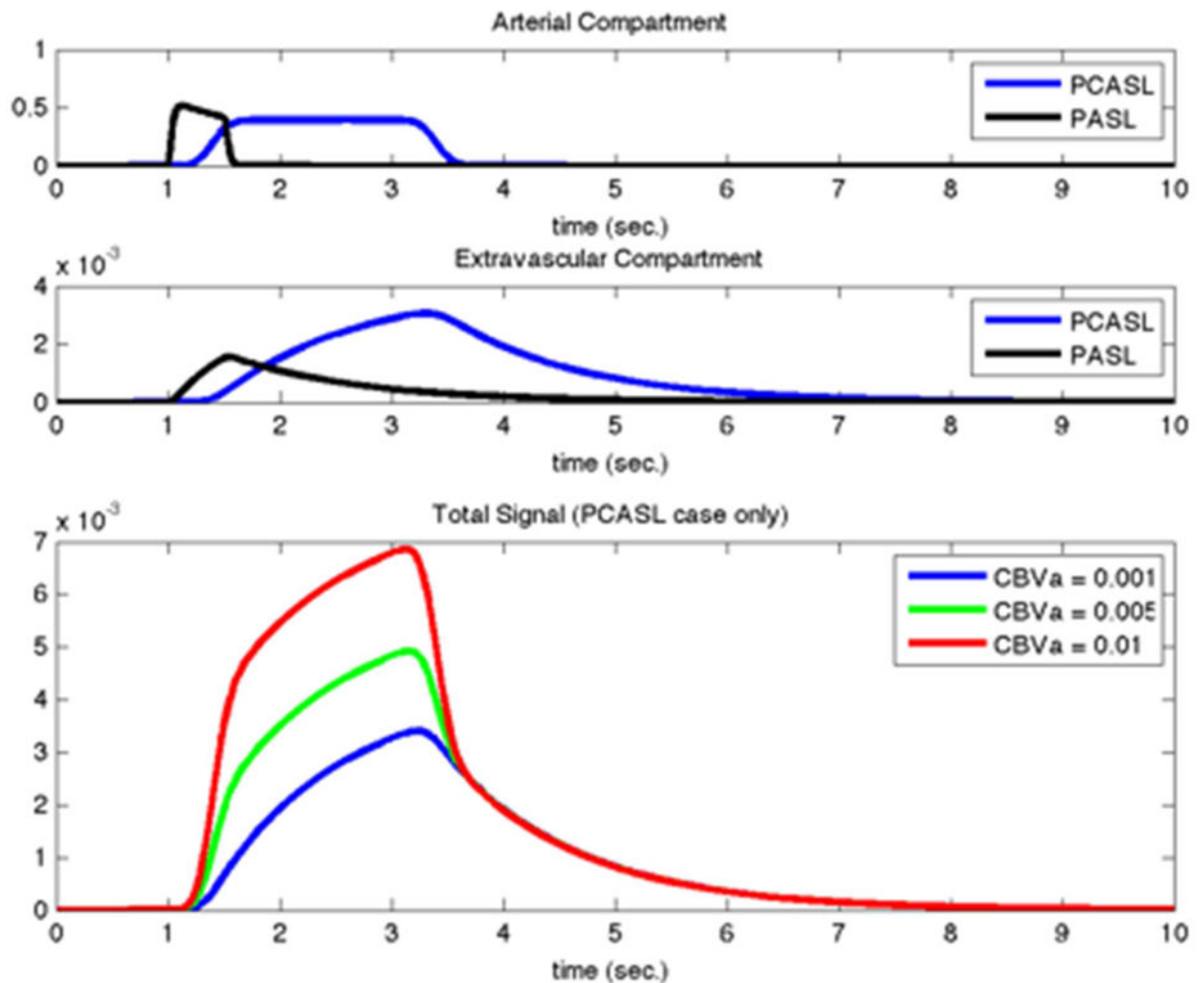


Figure 8. ASL signal models capture the concentration of the label in a voxel as they move through the arterial compartment into the extravascular compartment, using the two-compartment model (without the pass-thru artery) in the middle panel of figure 7. Generally, the observed signal is the sum of the two compartments, unless the arterial compartment is suppressed during the acquisition.

T₂ Relaxation Under Spin Tagging (TRUST)

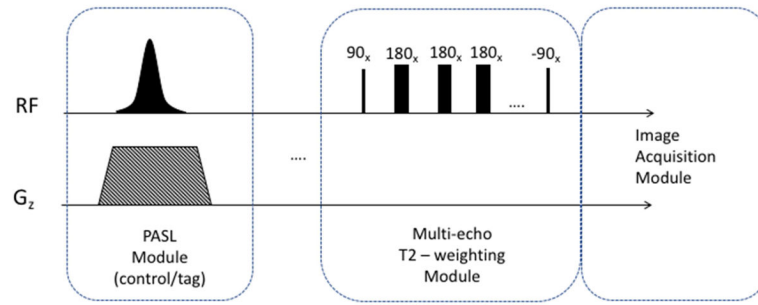
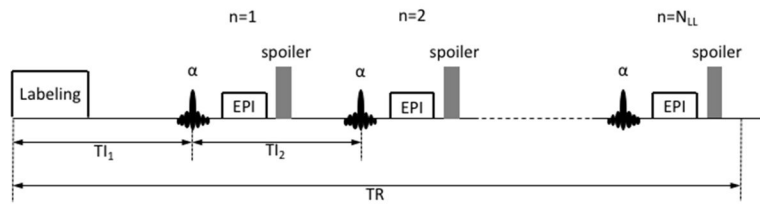


Figure 9.

The TRUST pulse sequence consists of a labeling module to isolate the venous inflow, followed by a T₂ weighting module to differentiate between oxygenated and deoxygenated blood.

Look-Locker Acquisition

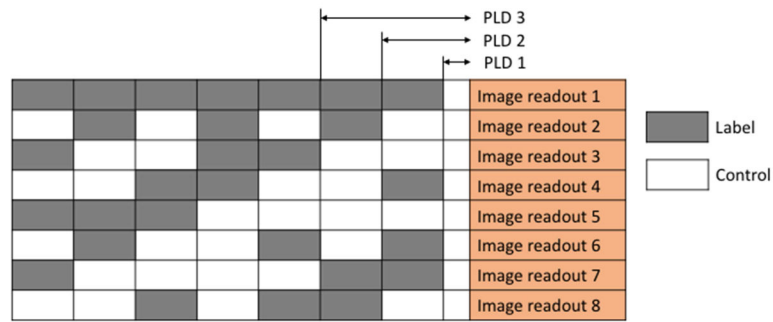


Guenter et al. 2001

Figure 10.

A Look-Locker ASL acquisition consisting of a labeling module immediately followed by a train of fast acquisitions to capture the inflow of the label into the arterial tree and its uptake by the extra vascular compartment.

Hadamard Encoding



Wells et al. 2010

Figure 11.

Bolus Arrival Time (Arterial Transit Time) information can be obtained by multiple ASL acquisitions with varying duration and delay of the labeling function. The Hadamard encoding sequence constitutes an efficient combination of timings in order to collect the ASL input function.

ASL fingerprinting signal generation

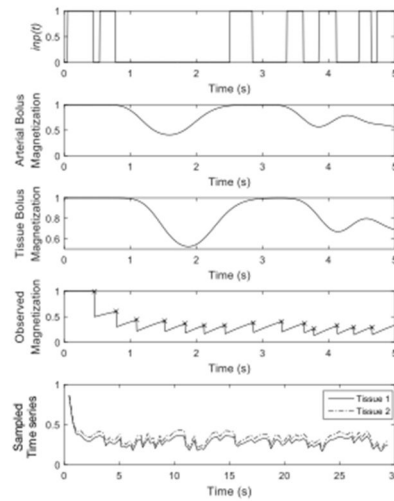


Figure 12.

ASL fingerprinting. A pseudo-random labeling scheme is used to generate an image time series whose signal is unique for a given combination of hemodynamic parameters. The top panel indicates a labeling function, the second panel shows the concentration of the label in the arterial compartment. Similarly, the third panel shows the concentration of the label in the extra-vascular compartment. The total magnetization (spin history) of the whole voxel is plotted in the fourth compartment. Finally, the bottom panel shows the observed time series from two different voxels.